MZ-TH/95-17
hep-ph/9508399
August 1995

Transverse Polarization of Top Quarks Produced in e^+e^--Annihilation at $O(\alpha_s)$

S. Groote*, J.G. Körner*

Institut für Physik, Johannes-Gutenberg-Universität
Staudingerweg 7, D-55099 Mainz, Germany.

ABSTRACT

We present the results of an $O(\alpha_s)$ calculation of the transverse polarization of top quarks produced in e^+e^--annihilation. In a first step we determine the transverse polarization of the top with regard to the hadron plane spanned by the $(q, \overline{q}, g)$ system. We then rotate the transverse components of the polarization to the lepton plane spanned by the (q, e^+, e^-) system. After azimuthal averaging we determine the three remaining inclusive transversely polarized structure functions. Together with the one-loop and Born term contributions they determine the $\sin\theta$ and $\sin 2\theta$ beam-quark polar angle dependence of the transverse polarization. We present analytic and numerical results for the polarized structure functions and the polar angle dependence of the transverse polarization. We briefly comment on the transverse polarization of bottom quarks produced in e^+e^--annihilation.

*Supported in part by the BMFT, FRG, under contract 06MZ566,
and by HUCAM, EU, under contract CHRX-CT94-0579

The recent discovery of the top quark at Fermilab in $p\bar{p}$-collisions provides the challenge and motivation to further investigate its production and decay characteristics in other processes. A very convenient tool in this regard is the proposed linear e^+e^--collider that has sufficient energy to produce top quark pairs. The produced top quarks in e^+e^--annihilations will be highly polarized. Furthermore they are so heavy that they decay before hadronizing. Thus the measurement of the polarization components of the produced top quarks is feasible through the study of spin-momentum correlations in top quark decay [1]. In this note we will be concerned with the transverse components of the top quark's polarization. The Born term contributions to the top quark's transverse polarization have been computed some time ago [2,3]. We shall present one-loop $O(\alpha_s)$ corrections to these results. We mention that in particular the transverse normal polarization has been widely discussed in the last few years because it is a T-odd observable and thus has implications for the possible observation of CP-violation in this process.

For the three-body process $(\gamma_V, Z) \to q(p_1) + \overline{q}(p_2) + g(p_3)$ we define a polarized hadron tensor according to ($q = p_1 + p_2 + p_3$)

$$H_{\mu\nu}(q, p_1, p_2, s) = \sum_{\overline{q},g \text{ spins}} \langle q\,\overline{q}\,g|j_\mu|0\rangle\langle 0|j_\nu^\dagger|q\,\overline{q}\,g\rangle \tag{1}$$

Note that the spin sum does not include the quark's spin which one wants to observe. The hadronic tensor $H_{\mu\nu}(q, p_1, p_2, s)$ can be decomposed into a number of spin dependent and spin independent structure functions which depend on q^2 and on the two energy variables $y = 1 - 2p_1{\cdot}q/q^2$ and $z = 1 - 2p_2{\cdot}q/q^2$. For our purposes it is convenient to work in terms of helicity structure functions which we shall sometimes refer to as rate functions.

In Table 1 we have listed a complete set of three-body helicity structure functions both in terms of the helicity and the Cartesian components of the hadron tensor. We have also listed the angular coefficients that multiply the rate functions after contraction of the hadron and the lepton tensor. The relative hadron-lepton orientation angles θ (polar) and χ (azimuthal) are defined in Fig. 1. In the following we shall refer to the plane spanned by $(q, \overline{q}, g)$ as the hadron plane and the plane spanned by (q, l^+, l^-) as the lepton plane. In this paper we restrict our analysis to the case of unpolarized e^+ and e^- beams. Longitudinal beam polarization effects can easily be incorporated into the analysis since

they come in with the same angular dependence as written down in Table 1 (see e.g. [2] and [4]). Transverse beam polarization effects introduce new angular dependencies which must be treated separately [4,5].

There are in general nine independent components of the hadron tensor each for the unpolarized case and for the three polarization directions. It is quite apparent that the three-particle hadron tensor $H_{\mu\nu}(q, p_1, p_2, s)$ posesses a very rich structure which can be resolved in terms of the angular dependence given in Table 1.

Let us start by listing the tree-graph contribution to the three-body hadron tensor. Here we limit our attention to the spin-dependent pieces. The spin-independent pieces are given in [5]. For the vector/vector (VV) and axial-vector/axial-vector (AA) contribution we obtain (using the abbreviation $\xi = 4m^2/q^2$)

$$\begin{aligned}
H^1_{\mu\nu} &:= \frac{1}{2}(H^{VV}_{\mu\nu} + H^{AA}_{\mu\nu}) \\
&= \frac{2im}{y^2z^2q^4}\Big[\, q^2(2-\xi)y^2\varepsilon(\mu\nu p_1 s) - q^2(4yz - 2\xi yz + 2y^2z - 2yz^2)\varepsilon(\mu\nu p_2 s) \\
&\quad + q^2(2y^2 - \xi y^2 - 2yz + 2\xi yz + \xi z^2)\varepsilon(\mu\nu p_3 s) \\
&\quad - 4y^2(p_{1\mu} + p_{3\mu})\varepsilon(\nu p_1 p_2 s) + 4y^2(p_{1\nu} + p_{3\nu})\varepsilon(\mu p_1 p_2 s) \\
&\quad + 4y(yp_{1\mu} + zp_{2\mu} + yp_{3\mu})\varepsilon(\nu p_2 p_3 s) - 4y(yp_{1\nu} + zp_{2\nu} + yp_{3\nu})\varepsilon(\mu p_2 p_3 s)\,\Big] \qquad (2) \\
H^2_{\mu\nu} &:= \frac{1}{2}(H^{VV}_{\mu\nu} - H^{AA}_{\mu\nu}) = \frac{2im}{y^2z^2q^4}\Big[\, q^2(\xi y^2 - 2yz + \xi yz + \xi z^2 + 4yz^2)\varepsilon(\mu\nu p_1 s) \\
&\quad - q^2\xi z(y-z)\varepsilon(\mu\nu p_2 s) + q^2\xi y(y-z)\varepsilon(\mu\nu p_3 s) \\
&\quad - 4yz(p_{1\mu} + p_{3\mu})\varepsilon(\nu p_1 p_2 s) + 4yz(p_{1\nu} + p_{3\nu})\varepsilon(\mu p_1 p_2 s) \\
&\quad - 4yz(p_{1\mu} - p_{2\mu} + p_{3\mu})\varepsilon(\nu p_1 p_3 s) + 4yz(p_{1\nu} - p_{2\nu} + p_{3\nu})\varepsilon(\mu p_1 p_3 s)\,\Big]. \qquad (3)
\end{aligned}$$

Note that in general $H^{VV}_{\mu\nu} \neq H^{AA}_{\mu\nu}$ and thereby $H^2_{\mu\nu} \neq 0$ in the massive quark case.

For the vector/axial-vector contributions we obtain

$$\begin{aligned}
H^3_{\mu\nu} &:= \frac{i}{2}(H^{VA}_{\mu\nu} - H^{AV}_{\mu\nu}) \\
&= \frac{2im}{y^2z^2q^4}\Big[- 4yz(p_3 s)(p_{1\mu}p_{2\nu} - p_{2\mu}p_{1\nu}) + 4yz((p_2 s) + (p_3 s))(p_{1\mu}p_{3\nu} - p_{3\mu}p_{1\nu}) \\
&\quad - q^2(\xi y^2 - 4yz + 2\xi yz + 2y^2 z + \xi z^2 + 4yz^2)(p_{1\mu}s_\nu - s_\mu p_{1\nu}) \\
&\quad - 2q^2yz^2(p_{2\mu}s_\nu - s_\mu p_{2\nu}) - q^2(\xi y^2 - 2yz + \xi yz + 2y^2 z)(p_{3\mu}s_\nu - s_\mu p_{3\nu})\,\Big] \qquad (4)
\end{aligned}$$

$$
\begin{aligned}
H^4_{\mu\nu} &:= \frac{1}{2}(H^{VA}_{\mu\nu} + H^{AV}_{\mu\nu}) \\
&= \frac{2m}{y^2z^2q^4}\Big[-q^2((\xi y^2 - 4yz + 2\xi yz + 2y^2z + \xi z^2 + 2yz^2)(p_2 s) \\
&\qquad +(-2y^2 + \xi y^2 - 2yz + 2\xi yz + 4y^2z + \xi z^2)(p_3 s))g_{\mu\nu} \\
&\quad -4y^2(p_3 s)(p_{1\mu}p_{2\nu} + p_{2\mu}p_{1\nu}) + 8yz(p_3 s)p_{2\mu}p_{2\nu} \\
&\quad -4y(z(p_2 s) + y(p_3 s))(p_{2\mu}p_{3\nu} + p_{3\mu}p_{2\nu}) + 2q^2y^2z(p_{1\mu}s_\nu + s_\mu p_{1\nu}) \\
&\quad +q^2(\xi y^2 - 4yz + 2\xi yz + 4y^2z + \xi z^2 + 2yz^2)(p_{2\mu}s_\nu + s_\mu p_{2\nu}) \\
&\quad +q^2(-2yz + \xi yz + 2y^2z + \xi z^2)(p_{3\mu}s_\nu + s_\mu p_{3\nu}) \Big]. \qquad (5)
\end{aligned}
$$

The spin-dependent pieces of the structure functions $H^1_{\mu\nu}$, $H^2_{\mu\nu}$ and $H^3_{\mu\nu}$ are antisymmetric in the Lorentz indices μ and ν, whereas the spin-dependent piece of $H^4_{\mu\nu}$ is symmetric. Note that all the spin-dependent tree-graph contributions $H^i_{\mu\nu}$ $(i = 1, 2, 3, 4)$ are proportional to the quark mass. This means that the transverse polarization vanishes in the mass zero limit. In the case of the alignment polarization, however, the mass factor is cancelled by the denominator mass factor in the covariant polarization vector s^ℓ_μ and thus the alignment polarization survives in the mass zero limit.

The three orthogonal polarization components of the quark are specified as s^ℓ_μ (alignment polarization along the momentum direction of the quark), $s^\perp_\mu$ (transverse polarization in the hadron plane with $s^\perp_\mu p^\mu_2 \leq 0$) and s^N_μ (transverse polarization normal to the hadron plane with $(s^\perp_\mu, s^N_\mu, s^\ell_\mu)$ forming a right-handed system in the quark's rest system). We then define polarized helicity structure functions H^m_α ($m = \perp, N, \ell$; in the following we shall mostly suppress the Lorentz index on s^m_μ) according to

$$
H^{i,m}_\alpha = H^i_\alpha(+s^m) - H^i_\alpha(-s^m), \qquad (6)
$$

where $\alpha = U, L, T, I, 9, F, A, 4, 5$ label the nine independent components of the hadron tensor (see Table 1). The unpolarized structure functions (not explicitly shown here) are given by

$$
H^i_\alpha = H^i_\alpha(+s^m) + H^i_\alpha(-s^m) \qquad (7)
$$

and are independent of the choice of s^m. An inspection of the tree-level expressions shows that not all of the polarized structure functions in Table 1 are populated (seven each for s^ℓ

and $s^\perp$ $(U, L, T, I, F, A, 9)$ and five for s^N $(4, 5, A, F, 9)$). The remaining structure would be populated by absorbtive and/or CP-violating contributions.

Our main interest in this paper is the transverse polarization of the quark relative to the lepton plane after integration over the relative azimuthal angle χ of the lepton and hadron planes. This constitutes a more inclusive polarization measure as compared to the full structure implied by Eqs. (2), (3), (4) and (5). It is apparent from Fig. 1 that the hadron plane is rotated into the lepton plane by the azimuthal angle χ. The alignment polarization structure function H_α^ℓ is not affected by this rotation whereas the transverse pieces are transformed according to

$$\begin{aligned} H_\alpha^{\perp\prime} &= \cos\chi H_\alpha^\perp - \sin\chi H_\alpha^N \\ H_\alpha^{N\prime} &= \sin\chi H_\alpha^\perp + \cos\chi H_\alpha^N, \end{aligned} \tag{8}$$

where the primed transverse polarization directions $s^{\perp\prime}$ and $s^{N\prime}$ now refer to the lepton plane. From the azimuthal χ-dependencies given in Table 1 and from Eq. (8) one can surmise that after the azimuthal integration

1. all transverse components $H_{U,L,T,F}^\perp$ and $H_{4,F}^N$ drop out,

2. there is a contribution *normal* to the lepton plane, i.e. $\sigma^{N\prime} \neq 0$, coming from the imaginary part of the Breit-Wigner resonance shape via (γ, Z) interference. This contribution is of order $O(Im\,\chi_z(q^2)/\,Re\,\chi_z(q^2))$ and can thus safely be neglected for top pair production. For example, in the threshold region of top pair production, this transverse normal polarization effect is already quite small since the factor $Im\,\chi_z/\,Re\,\chi_z$ is approximately 0.1% and decreases further with a $1/q^2$ power fall-off behaviour. We shall nevertheless explicitly include this part in the following for the sake of completeness and also because of the fact that this interference effect is one of the sources of transverse normal polarization of b-quarks from Z-decays. A further sizable contribution to $\sigma^{N\prime}$ comes from the imaginary part of the one-loop graph which will be discussed later on.

3. $H_I^\perp$ and H_5^N contribute with the weight factor $\frac{3}{2\sqrt{2}}\sin 2\theta$, and $H_A^\perp$ and H_9^N contribute with the factor $\frac{3}{\sqrt{2}}\sin\theta$ to the transverse polarization *in* the lepton plane.

For definiteness, we present our transverse polarization results in terms of polarization cross sections. One has

$$\frac{d\sigma^{\perp'}}{d\cos\theta\, dy\, dz} = -\frac{3}{2\sqrt{2}}\sin 2\theta\, g_{14}\frac{d\sigma_I^{4\perp'}}{dy\, dz} - \frac{3}{\sqrt{2}}\sin\theta\left(g_{41}\frac{d\sigma_A^{1\perp'}}{dy\, dz} + g_{42}\frac{d\sigma_A^{2\perp'}}{dy\, dz}\right), \tag{9}$$

$$\frac{d\sigma^{N'}}{d\cos\theta\, dy\, dz} = -\frac{3}{\sqrt{2}}\sin\theta\, g_{43}\frac{d\sigma_A^{3N'}}{dy\, dz}, \tag{10}$$

where, in terms of the hadron-plane helicity structure functions $H_\alpha^{i,m}$ defined in Eq. (6), one has

$$\frac{d\sigma_\alpha^{i,m'}}{dy\, dz} = \frac{\pi\alpha^2 v}{3q^4}\left\{\frac{q^2}{16\pi^2 v}H_\alpha^{i,m'}\right\} \tag{11}$$

with

$$H_I^{4\perp'} = \frac{1}{2}(H_I^{4\perp} + H_5^{4N}) \qquad H_A^{1,2\,\perp'} = \frac{1}{2}(H_A^{1,2\,\perp} + H_9^{1,2\,N}) \qquad H_A^{3N'} = \frac{1}{2}(H_A^{3N} - H_9^{3\perp}). \tag{12}$$

In Eq. (11) we have split up the three-body phase space factor into the two-body phase space factor $\pi\alpha^2 v/3q^4$ and the relative two-body/three-body phase space factor $q^2/16\pi^2 v$ in order to facilitate the comparison with the respective two-body loop and Born term contributions.

The respective polarization cross sections represent components of the unnormalized polarization vector. The corresponding components of the normalized polarization vector are then obtained by dividing by the unpolarized cross section given by

$$\begin{aligned}\frac{d\sigma}{d\cos\theta\, dy\, dz} &= \frac{3}{8}(1+\cos^2\theta)\left(g_{11}\frac{d\sigma_U^1}{dy\, dz} + g_{12}\frac{d\sigma_U^2}{dy\, dz}\right) \\ &\quad + \frac{3}{4}\sin^2\theta\left(g_{11}\frac{d\sigma_L^1}{dy\, dz} + g_{12}\frac{d\sigma_L^2}{dy\, dz}\right) + \frac{3}{4}\cos\theta g_{44}\frac{d\sigma_F^4}{dy\, dz},\end{aligned} \tag{13}$$

where, in analogy with Eq. (11), one has

$$\frac{d\sigma_\alpha^i}{dy\, dz} = \frac{\pi\alpha^2 v}{3q^4}\left\{\frac{q^2}{16\pi^2 v}H_\alpha^i\right\}. \tag{14}$$

The unpolarized cross section results are taken from [5,6] and will not be listed explicitly in this paper.

In Eqs. (9), (10) and (13), we have perused the electro-weak coupling parameters

$$\begin{aligned}
g_{11} &= Q_f^2 - 2Q_f v_e v_f \, Re\,\chi_Z + (v_e^2+a_e^2)(v_f^2+a_f^2)|\chi_Z|^2, \\
g_{12} &= Q_f^2 - 2Q_f v_e v_f \, Re\,\chi_Z + (v_e^2+a_e^2)(v_f^2-a_f^2)|\chi_Z|^2, \\
g_{13} &= -2Q_f v_e a_f \, Im\,\chi_Z, \\
g_{14} &= 2Q_f v_e a_f \, Re\,\chi_Z - 2(v_e^2+a_e^2) v_f a_f |\chi_Z|^2, \\
g_{41} &= 2Q_f a_e v_f \, Re\,\chi_Z - 2v_e a_e (v_f^2+a_f^2)|\chi_Z|^2, \\
g_{42} &= 2Q_f a_e v_f \, Re\,\chi_Z - 2v_e a_e (v_f^2-a_f^2)|\chi_Z|^2, \\
g_{43} &= 2Q_f a_e a_f \, Im\,\chi_Z, \\
g_{44} &= -2Q_f a_e a_f \, Re\,\chi_Z + 4 v_e a_e v_f a_f |\chi_Z|^2
\end{aligned} \tag{15}$$

with

$$\chi_Z(q^2) = \frac{g M_Z^2 q^2}{q^2 - M_Z^2 + i M_Z \Gamma_Z}, \quad g = \frac{G_F}{8\sqrt{2}\pi\alpha} \approx 4.49 \cdot 10^{-5} \mathrm{GeV}^{-2}. \tag{16}$$

The Standard Model values of the electro-weak coupling constants are given by

$$\begin{aligned}
v_e &= -1 + 4\sin^2\theta_W, \quad a_e = -1 \quad \text{for leptons,} \\
v_f &= 1 - \frac{8}{3}\sin^2\theta_W, \quad a_f = 1 \quad \text{for up-type quarks } (Q_f = \tfrac{2}{3}), \text{ and} \\
v_f &= -1 + \frac{4}{3}\sin^2\theta_W, \quad a_f = -1 \quad \text{for down-type quarks } (Q_f = -\tfrac{1}{3}).
\end{aligned} \tag{17}$$

It is quite instructive to perform the above inclusive analysis more directly using the covariant decomposition of the relevant inclusive hadron tensor. One has

$$\begin{aligned}
&\frac{q^2}{16\pi^2 v}\int_0^{2\pi}\frac{d\chi}{2\pi}\int_{z_-(y)}^{z_+(y)} dz\, H_{\mu\nu}(q,p_1,p_2,s) \;= \\
&= \boldsymbol{-\hat{g}_{\mu\nu} H_1^{pc} + \hat{p}_{1\mu}\hat{p}_{1\nu} H_2^{pc} + i\varepsilon(\mu\nu p_1 q) H_3^{pv}} + q_\mu q_\nu H_4^{pc} + (q_\mu p_{1\nu} + q_\nu p_{1\mu}) H_5^{pc} \\
&\quad + (q\cdot s)\Big[\boldsymbol{-\hat{g}_{\mu\nu} G_1^{pv} + \hat{p}_{1\mu}\hat{p}_{1\nu} G_2^{pv} + i\varepsilon(\mu\nu p_1 q) G_3^{pc}} + q_\mu q_\nu G_4^{pv} + (q_\mu p_{1\nu} + q_\nu p_{1\mu}) G_5^{pv}\Big] \\
&\quad \boldsymbol{+(s_\mu \hat{p}_{1\nu} + s_\nu \hat{p}_{1\mu}) G_6^{pv}} + (s_\mu q_\nu + s_\nu q_\mu) G_7^{pv} \boldsymbol{+ i\varepsilon(\mu\nu q s) G_8^{pc} + i\varepsilon(\mu\nu \hat{p}_1 s) G_9^{pc}} \\
&\quad \boldsymbol{+ i(s_\mu \hat{p}_{1\nu} - s_\nu \hat{p}_{1\mu}) G_{10}^{pv}} + i(s_\mu q_\nu - s_\nu q_\mu) G_{11}^{pv} \\
&\quad \boldsymbol{+(\hat{p}_{1\mu}\varepsilon(\nu q p_1 s) + \hat{p}_{1\nu}\varepsilon(\mu q p_1 s)) G_{12}^{pc}} + (q_\mu \varepsilon(\nu q p_1 s) + q_\nu \varepsilon(\mu q p_1 s)) G_{13}^{pc}.
\end{aligned} \tag{18}$$

The spin vector s_μ now refers to any *fixed* space coordinate system. In particular, the fixed system should not make reference to the hadron plane since one is integrating over

the relative lepton-hadron azimuth in the inclusive measure Eq. (18). For our purposes it is most convenient to choose the lepton system $(x', y', z'(= z))$ as the reference system for the spin vector with the electron momentum pointing in the negative x'-direction, i.e. Eq. (18) should be read with the replacement $s_\mu \to s'_\mu$. There are altogether five spin-independent and 13 spin-dependent structure functions. Of these only the eleven boldfaced contribute to e^+e^--annihilation for zero lepton mass. As mentioned before, the remaining seven structure functions do not vanish by any means but are of no interest in this reaction since they cannot be probed in the zero lepton mass case. It is for this reason that we have written the covariants in Eq. (18) in terms of the four-transverse objects $\hat{g}_{\mu\nu} = g_{\mu\nu} - q_\mu q_\nu/q^2$ and $\hat{p}_{1\mu} = p_{1\mu} - (p_1 \cdot q)q_\mu/q^2$ so that the invariants separate into the two mentioned categories. Also the invariant structure functions G_8 and G_9 have been defined such that only G_8 is contributed to by *transversely* polarized quarks. For quick identification, the invariants carry a superscript (*pc*: parity conserving; *pv*: parity violating) according to whether they are fed by the parity conserving VV, AA or by the parity violating VA products of the hadron currents. This superscript will be dropped in the following. Let us finally mention that G_{10}, G_{11}, G_{12} and G_{13} are so-called T-odd structure functions. The tree-graph only contributes to the T-odd structure functions G_{10} and G_{11}.

The transverse polarization in the lepton plane is given in terms of the two structure functions G_6 and G_8. These can easily be projected out by contracting Eq. (18) (with $s_\mu \to s'_\mu$) on the r.h.s. with $(s_\mu^{\perp\prime}\hat{p}_{1\nu} + s_\nu^{\perp\prime}\hat{p}_{1\mu})$ and $\varepsilon(\mu\nu q s^{\perp\prime})$, respectively. On the l.h.s. of Eq. (18) the contractions can be done directly on the integrand since integration and contraction commute. In this way we obtain

$$-\sqrt{2}p_{1z}G_6^4 = \frac{q^2}{16\pi^2 v}\int\frac{d\chi}{2\pi}\int dz\frac{1}{2}(H_I^{4\perp} + H_5^{4N}), \tag{19}$$

$$\sqrt{2}\sqrt{q^2}G_8^{1,2} = \frac{q^2}{16\pi^2 v}\int\frac{d\chi}{2\pi}\int dz\frac{1}{2}(H_A^{1,2\,\perp} + H_9^{1,2\,N}). \tag{20}$$

The transverse normal structure function G_{10} is projected out by contraction with $(s_\mu^{N\prime}\hat{p}_{1\nu} - s_\nu^{N\prime}\hat{p}_{1\mu})$. One obtains

$$\sqrt{2}p_{1z}G_{10}^3 = \frac{q^2}{16\pi^2 v}\int\frac{d\chi}{2\pi}\int dz\frac{1}{2}(H_A^{3N} - H_9^{3\perp}). \tag{21}$$

Let us now present our results for the integrated three-body tree-graph polarized

rate functions in terms of the rate functions

$$\hat{H}_\alpha^{i,m'}(tree) = \frac{q^2}{16\pi^2 v}\int dy\, dz\, H_\alpha^{i,m'}(y,z), \tag{22}$$

where the hat symbol on the structure function has been added to remind one-self that one is dealing with an integrated three-body structure function. The complete $O(\alpha_s)$ contribution is then given by adding in the $O(\alpha_s)$ one-loop contributions (taken from [6]). One has

$$\hat{H}_\alpha^{i,m'}(\alpha_s) = \hat{H}_\alpha^{i,m'}(tree) + H_\alpha^{i,m'}(loop). \tag{23}$$

Note that the IR-singularity contained in the integrated tree-graph contribution exactly cancels the IR-singularity in the one-loop contribution such that the sum of the two terms in Eq. (23) is IR-finite. We have regularized the IR-singularity by introducing a (small) gluon mass. The gluon mass regulator is of no concern when calculating the tree-graph matrix elements Eqs. (2–5) but only serves to slightly deform the phase-space away from the IR-singularity. One has

$O(\alpha_s)$ real part:

$$\begin{aligned}
\hat{H}_I^{4\perp\prime}(\alpha_s) &= \frac{1}{2}(\hat{H}_I^{4\perp}(\alpha_s) + \hat{H}_5^{4N}(\alpha_s)) \\
&= -\frac{\alpha_s}{\pi}N_C C_F \frac{m\sqrt{q^2}}{2\sqrt{2}v}\Big[(1-\sqrt{\xi})(24 - 7\sqrt{\xi} + \frac{3}{2}\xi) + 4v^2 t_{11} \\
&\quad +4v^2 t_{10} - 2(2-\xi)v(t_7 - t_8) + (8 + \frac{7}{2}\xi)t_6 \\
&\quad -(21+2\xi)vt_3 - \frac{1}{8}(4-\xi)(10+3\xi)(t_1 - t_2)\Big] \qquad (24) \\
\hat{H}_A^{1\perp\prime}(\alpha_s) &= \frac{1}{2}(\hat{H}_A^{1\perp}(\alpha_s) + \hat{H}_9^{1N}(\alpha_s)) \\
&= -\frac{\alpha_s}{\pi}N_C C_F \frac{m\sqrt{q^2}}{4\sqrt{2}v}\Big[(8-3\xi)v + 16vt_{12} + 8vt_{10} \\
&\quad +4(2-\xi)(t_8 - t_9) - (8+\xi)t_5 \\
&\quad +(1-\sqrt{\xi})(8 - 2\sqrt{\xi} - \xi)t_4 - (36 - 19\xi + \frac{3}{2}\xi^2)t_3\Big] \qquad (25) \\
\hat{H}_A^{2\perp\prime}(\alpha_s) &= \frac{1}{2}(\hat{H}_A^{2\perp}(\alpha_s) + \hat{H}_9^{2N}(\alpha_s)) \\
&= \frac{\alpha_s}{\pi}N_C C_F \frac{m\sqrt{q^2}}{4\sqrt{2}v}\Big[(20-3\xi)v - 16vt_{12} - 8vt_{10} \\
&\quad -4(2-\xi)(t_8 - t_9) + \xi t_5 - \xi(1-\sqrt{\xi})t_4 + (16 - 7\xi - \frac{3}{2}\xi^2)t_3\Big] \qquad (26) \\
\hat{H}_A^{3N\prime}(\alpha_s) &= \frac{1}{2}(\hat{H}_A^{3N}(\alpha_s) - \hat{H}_9^{3\perp}(\alpha_s))
\end{aligned}$$

$$
\begin{aligned}
= \; & \frac{\alpha_s}{\pi} N_C C_F \frac{m\sqrt{q^2}}{2\sqrt{2}v}\Big[(1-\sqrt{\xi})(10-3\sqrt{\xi}+\frac{3}{2}\xi) - 4v^2 t_{11} \\
& -4v^2 t_{10} + 2(2-\xi)v(t_7 - t_8) - (4-\frac{13}{2}\xi)t_6 \\
& +(1-6\xi)v t_3 - (3-\frac{1}{4}\xi-\frac{3}{8}\xi^2)(t_1-t_2)\Big] \qquad (27)
\end{aligned}
$$

Closed form expressions for the integrals t_i $(i = 1, \ldots, 12)$ appearing in Eqs. (24)–(27) can be found in the Appendix.

What remains is to write down the corresponding Born term expressions. The easiest way to obtain these is to directly read off the relevant covariant structure functions G^i_j from the two-body hadron tensor $H^i_{\mu\nu}$. One has

Born terms:

$$
-\sqrt{2}p_{1z}G^4_6 \;=\; H_I^{4\perp\prime} \;=\; \frac{1}{2}(H_I^{4\perp} + H_5^{4N}) \;=\; -\sqrt{2}N_C m v\sqrt{q^2} \qquad (28)
$$

$$
\sqrt{2}\sqrt{q^2}G^{1,2}_8 \;=\; H_A^{1,2\,\perp\prime} \;=\; \frac{1}{2}(H_A^{1,2\,\perp} + H_9^{1,2\,N}) \;=\; \sqrt{2}N_C m\sqrt{q^2} \qquad (29)
$$

$$
\sqrt{2}p_{1z}G^3_{10} \;=\; H_A^{3N\prime} \;=\; \frac{1}{2}(H_A^{3N} - H_9^{3\perp}) \;=\; \sqrt{2}N_C m v\sqrt{q^2} \qquad (30)
$$

As mentioned before, the contribution of $H_A^{3N'}$ can be neglected for $t\bar{t}$-production as the $t\bar{t}$-threshold is quite far away from the Z-pole.

The last missing piece of information is the $O(\alpha_s)$ contribution of the imaginary part of the one-loop contribution to $\frac{1}{2}(H_I^{iN} - H_5^{i\perp}) \propto G^i_{12}$ $(i = 1, 2)$, $\frac{1}{2}(H_A^{4\perp} - H_9^{4N}) \propto G^4_{10}$ and $\frac{1}{2}(H_I^{3\perp} + H_5^{3N}) \propto G^3_6$. These can be read off from the one-loop result given e.g. in [6].

$O(\alpha_s)$ imaginary part:

$$
\begin{aligned}
-\sqrt{2}p_{1z}G^3_6 \;=\; \hat{H}_I^{3\perp\prime}(\alpha_s) \;&=\; \frac{1}{2}(\hat{H}_I^{3\perp}(\alpha_s) + \hat{H}_5^{3N}(\alpha_s)) \\
&=\; -\frac{\alpha_s}{\pi}N_C C_F \frac{m\sqrt{q^2}}{2\sqrt{2}}\pi(1+\xi) \qquad (31) \\
-2\sqrt{2}m p_{1z}^2 G^{1,2}_{12} \;=\; \hat{H}_I^{1,2\,N\prime}(\alpha_s) \;&=\; \frac{1}{2}(\hat{H}_I^{1,2\,N}(\alpha_s) - \hat{H}_5^{1,2\,\perp}(\alpha_s)) \\
&=\; -\frac{\alpha_s}{\pi}N_C C_F \frac{m\sqrt{q^2}}{2\sqrt{2}}\pi v \qquad (32) \\
\sqrt{2}p_{1z}G^4_{10} \;=\; \hat{H}_A^{4N\prime}(\alpha_s) \;&=\; \frac{1}{2}(\hat{H}_A^{4N}(\alpha_s) - \hat{H}_9^{4\perp}(\alpha_s)) \\
&=\; \frac{\alpha_s}{\pi}N_C C_F \frac{m\sqrt{q^2}}{2\sqrt{2}}\pi(1+\xi). \qquad (33)
\end{aligned}
$$

The imaginary parts of the one-loop contribution for $\hat{H}_I^{1,2\,N'}$ and $\hat{H}_A^{4N'}$ agree with the results given in [2]. The contribution to the transverse perpendicular structure function $\hat{H}_I^{3\perp'}$ has not been considered in [2]. Of course, in case of $t\bar{t}$-production, this contribution can again safely be neglected. The angular factors entering the two-body polarization cross sections can be read off from Table 1. One obtains

$$\frac{d\sigma^{\perp'}}{d\cos\theta} = \frac{\pi\alpha^2 v}{3q^4}\left\{ -\frac{3}{2\sqrt{2}}\sin 2\theta\, g_{13}\hat{H}_I^{3\perp'}\right\} \tag{34}$$

$$\frac{d\sigma^{N'}}{d\cos\theta} = \frac{\pi\alpha^2 v}{3q^4}\left\{ -\frac{3}{2\sqrt{2}}\sin 2\theta(g_{11}\hat{H}_I^{1N'} + g_{12}\hat{H}_I^{2N'}) - \frac{3}{\sqrt{2}}\sin\theta\, g_{44}\hat{H}_A^{4N'}\right\}. \tag{35}$$

We are now in the position to determine the polar angle dependence of the two transverse polarizations by adding up the $O(\alpha_s^0)$ Born term contribution and the $O(\alpha_s)$ loop and tree contributions according to the ratio expressions

$$P^{\perp'}(\cos\theta) = \frac{d\sigma^{\perp'}(Born + loop + tree)/d\cos\theta}{d\sigma(Born + loop + tree)/d\cos\theta} \tag{36}$$

$$P^{N'}(\cos\theta) = \frac{d\sigma^{N'}(Born + loop + tree)/d\cos\theta}{d\sigma(Born + loop + tree)/d\cos\theta}. \tag{37}$$

The polarized expressions constitute mean polarizations over the full (y, z)-Dalitz plot region.

In Fig. 2a we show our results for the $O(\alpha_s^0) + O(\alpha_s)$ perpendicular polarization of the top quark for three repesentative c.m. energies, where the lowest energy $\sqrt{q^2} =$ 360 GeV is chosen to lie far enough above the nominal threshold value of $\sqrt{q^2} = 348$ GeV for a perturbative calculation to make sense. The perpendicular polarization is positive and large. It decreases with increasing energy because of the aforementioned $m/\sqrt{q^2}$ dependence of the transverse polarization. We also show the Born term results (dotted lines). It is apparent that the $O(\alpha_s)$ corrections to the Born term result are negative and small. At $\sqrt{q^2} = 1000$ GeV they can amount up to $\simeq 10\%$ depending on the value of the polar angle θ. Close to threshold the radiative corrections have become so small that they are hardly visible on the scale of the figure. The perpendicular polarization is positive over the whole angular range indicating that the $\sin\theta$ contribution overwhelms the $\sin 2\theta$ contribution, in particular close to threshold.

In Fig. 2b we show the polar angle dependence of the normal polarization, again for the three energies $\sqrt{q^2} = 360$ GeV, 500 GeV and 1000 GeV. The polarization peaks

towards the larger θ-values, where the electron and the top quark are in different hemispheres. The normal polarization is mainly an $O(\alpha_s)$ effect coming from the imaginary part of the $O(\alpha_s)$ vertex correction. The corresponding $O(\alpha_s^0)$ Born term contributions are not drawn since they are so small that they cannot be discerned from the line of the abscissa. Again the $\sin\theta$ contribution dominates over the $\sin 2\theta$ contribution because of the presence of the threshold power $v = \sqrt{1-\xi}$ in $\hat{H}_I^{1,2\,N'}$ (see Eq. (32)). The linear $m/\sqrt{q^2}$ power behaviour of the transverse polatization is clearly evident in Fig. 2b in as much as the polarization decreases with increasing energy over most of the $\cos\theta$-range.

In Fig. 3 we show the transverse polarization of the bottom quark on the Z-peak. The perpendicular polarization (Fig. 3a) is small but still sizeable which shows that one cannot always neglect bottom quark mass effects. Also the radiative corrections are quite large in this case. In the case of the bottom quark the $\sin 2\theta$ term is the dominating term in the polar angle distribution. In fact, when averaged over $\cos\theta$, the perpendicular polarization can be seen to be quite small ($\langle P^{\perp'}\rangle \simeq 0.61\%$).

The transverse normal polarization of bottom quarks in $Z \to b\bar{b}$ is shown in Fig. 3b. As it turns out both contributions from the imaginary part of the loop and the Breit-Wigner interference term are of almost equal importance with a slight dominance of the Breit-Wigner contribution proportional to $\sin\theta$. We have taken a bottom quark mass of $m_b = 4.83$ GeV [7] for the curves in Fig. 3. If one uses a running bottom quark mass $\overline{m_b}(M_z) = 2.69$ GeV as in our previous works [6,8], the transverse polarization is reduced by a factor of approximately $m_b/\overline{m_b}(M_z) \simeq 1.8$.

Acknowledgement: We would like to thank K.G. Chetyrkin, K. Melnikov and M.M. Tung for helpful discussions.

Appendix

It is convenient to define the mass dependent variables $a := 2+\sqrt{\xi}$, $b := 2-\sqrt{\xi}$ and $w := \sqrt{(1-\sqrt{\xi})/(1+\sqrt{\xi})}$. The integrals $t_1, \ldots, t_{12}$ appearing in Eqs. (24)–(27) are then given by

$$t_1 := \ln\left(\frac{2\xi\sqrt{\xi}}{b^2(1+\sqrt{\xi})}\right), \quad t_2 := \ln\left(\frac{2\sqrt{\xi}}{1+\sqrt{\xi}}\right) \quad \Rightarrow \quad t_1 - t_2 = \ln\left(\frac{\xi}{b^2}\right) \tag{A1}$$

$$t_3 := \ln\left(\frac{1+v}{1-v}\right) \tag{A2}$$

$$t_4 := \mathrm{Li}_2(w) - \mathrm{Li}_2(-w) + \mathrm{Li}_2(\frac{a}{b}w) - \mathrm{Li}_2(-\frac{a}{b}w) \tag{A3}$$

$$\begin{aligned} t_5 := {} & \frac{1}{2}\ln\left(\frac{\sqrt{\xi}(2+\sqrt{\xi})}{4(1+\sqrt{\xi})}\right)\ln\left(\frac{1+v}{1-v}\right) + \mathrm{Li}_2\left(\frac{2\sqrt{\xi}}{a(1+w)}\right) - \mathrm{Li}_2\left(\frac{2\sqrt{\xi}}{a(1-w)}\right) + \\ & + \mathrm{Li}_2\left(\frac{1+w}{2}\right) - \mathrm{Li}_2\left(\frac{1-w}{2}\right) + \mathrm{Li}_2\left(\frac{a(1+w)}{4}\right) - \mathrm{Li}_2\left(\frac{a(1-w)}{4}\right) \end{aligned} \tag{A4}$$

$$\begin{aligned} t_6 := {} & \ln^2(1+w) + \ln^2(1-w) + \ln\left(\frac{2+\sqrt{\xi}}{8}\right)\ln(1-w^2) + \\ & + \mathrm{Li}_2\left(\frac{2\sqrt{\xi}}{a(1+w)}\right) + \mathrm{Li}_2\left(\frac{2\sqrt{\xi}}{a(1-w)}\right) - 2\mathrm{Li}_2\left(\frac{2\sqrt{\xi}}{a}\right) + \\ & + \mathrm{Li}_2\left(\frac{1+w}{2}\right) + \mathrm{Li}_2\left(\frac{1-w}{2}\right) - 2\mathrm{Li}_2\left(\frac{1}{2}\right) + \\ & + \mathrm{Li}_2\left(\frac{a(1+w)}{4}\right) + \mathrm{Li}_2\left(\frac{a(1-w)}{4}\right) - 2\mathrm{Li}_2\left(\frac{a}{4}\right) \end{aligned} \tag{A5}$$

$$\begin{aligned} t_7 := {} & 2\ln\left(\frac{1-\xi}{2\xi}\right)\ln\left(\frac{1+v}{1-v}\right) - \mathrm{Li}_2\left(\frac{2v}{(1+v)^2}\right) + \mathrm{Li}_2\left(-\frac{2v}{(1-v)^2}\right) + \\ & - \frac{1}{2}\mathrm{Li}_2\left(-\left(\frac{1+v}{1-v}\right)^2\right) + \frac{1}{2}\mathrm{Li}_2\left(-\left(\frac{1-v}{1+v}\right)^2\right) + \\ & + \mathrm{Li}_2\left(\frac{2w}{1+w}\right) - \mathrm{Li}_2\left(-\frac{2w}{1-w}\right) - 2\mathrm{Li}_2\left(\frac{w}{1+w}\right) + 2\mathrm{Li}_2\left(-\frac{w}{1-w}\right) + \\ & + \mathrm{Li}_2\left(\frac{2aw}{b+aw}\right) - \mathrm{Li}_2\left(-\frac{2aw}{b-aw}\right) - 2\mathrm{Li}_2\left(\frac{aw}{b+aw}\right) + 2\mathrm{Li}_2\left(-\frac{aw}{b-aw}\right) \end{aligned} \tag{A6}$$

$$t_8 := \ln\left(\frac{\xi}{4}\right)\ln\left(\frac{1+v}{1-v}\right) + \mathrm{Li}_2\left(\frac{2v}{1+v}\right) - \mathrm{Li}_2\left(-\frac{2v}{1-v}\right) - \pi^2 \tag{A7}$$

$$\begin{aligned} t_9 := {} & 2\ln\left(\frac{2(1-\xi)}{\sqrt{\xi}}\right)\ln\left(\frac{1+v}{1-v}\right) + 2\left(\mathrm{Li}_2\left(\frac{1+v}{2}\right) - \mathrm{Li}_2\left(\frac{1-v}{2}\right)\right) + \\ & + 3\left(\mathrm{Li}_2\left(-\frac{2v}{1-v}\right) - \mathrm{Li}_2\left(\frac{2v}{1+v}\right)\right) \end{aligned} \tag{A8}$$

$$t_{10} := \ln\left(\frac{4}{\xi}\right), \quad t_{11} := \ln\left(\frac{4(1-\sqrt{\xi})^2}{\xi}\right), \quad t_{12} := \ln\left(\frac{4(1-\xi)}{\xi}\right) \tag{A9}$$

References

[1] R.H. Dalitz and G.R. Goldstein, Phys. Rev. **D45** (1992) 1531;
W. Bernreuther, J.P. Ma and T. Schröder, Phys. Lett. **B297** (1992) 318;
W. Bernreuther, O. Nachtmann, P. Overmann and T. Schröder,
Nucl. Phys. **B388** (1992) 53; (E) Nucl. Phys. **B406** (1993) 516;
A. Czarnecki, M. Jezabek, J.G. Körner and J.H. Kühn,
Phys. Rev. Lett. **73** (1994) 384;
A. Czarnecki and M. Jezabek, Nucl. Phys. **B427** (1994) 3

[2] J.H. Kühn, A. Reiter and P.M. Zerwas, Nucl. Phys. **B272** (1986) 560

[3] M. Anselmino, P. Kroll and B. Pire, Phys. Lett. **B167** (1986) 113

[4] J.G. Körner and D.H. Schiller, preprint DESY-81-043 (1981);
H.A. Olson, P. Osland and I. Øverbø, Nucl. Phys. **B171** (1980) 209

[5] S. Groote, J.G. Körner and M.M. Tung, to be published

[6] J.G. Körner, A. Pilaftsis and M.M. Tung, Z. Phys. **C63** (1994) 575

[7] M.B. Voloshin, Int. J. of Mod. Phys. **A10** (1995) 2865

[8] S. Groote, J.G. Körner and M.M. Tung, "Longitudinal Contribution to the Alignment Polarization of Quarks Produced in e^+e^--Annihilation: An $O(\alpha_s)$-Effect",
Mainz preprint MZ-TH/95-09, hep-ph 9507222, to be published in Z. Phys. C

Table Captions

Tab. 1: Independent helicity components of the hadron tensor $H_{\mu\nu}$ in the spherical basis (column 2) and in the Cartesian basis (column 3). Column 4 gives the respective angular coefficients that determine the lepton-hadron correlations

Figure Captions

Fig. 1: Definition of the polar angle θ and azimuthal angle χ decribing the relative orientation between lepton plane and hadron plane

Fig. 2: Transverse polarization for the top-quark with mass $m_t = 174$ GeV and running coupling constant α_s, $\alpha_s(M_Z) = 0.118$) at three different energies ($\sqrt{q^2} = 360$ GeV (full line), 500 GeV (dashed) and 1000 GeV (dash-dotted)). Born term results drawn as dotted lines
(a) perpendicular polarization (b) normal polarization

Fig. 3: Transverse polarization for the bottom-quark on the Z-peak (with bottom mass set to $m_b = 4.83$ GeV [7] and $\alpha_s(M_Z) = 0.118$).
Full line: $O(\alpha_s^0) + O(\alpha_s)$; dotted line: Born term result
(a) perpendicular polarization (b) normal polarization

	spherical components	Cartesian components	angular factors
H_U	$H_{++} + H_{--}$	$H_{11} + H_{22}$	$\frac{3}{8}(1 + \cos^2\theta)$
H_L	H_{00}	H_{33}	$\frac{3}{4}\sin^2\theta$
H_T	$\frac{1}{2}(H_{+-} + H_{-+})$	$\frac{1}{2}(-H_{11} + H_{22})$	$\frac{3}{4}\sin^2\theta\cos 2\chi$
H_I	$\frac{1}{4}(H_{+0} + H_{0+} - H_{-0} - H_{0-})$	$\frac{-1}{2\sqrt{2}}(H_{31} + H_{13})$	$\frac{-3}{2\sqrt{2}}\sin 2\theta\cos\chi$
H_9	$-\frac{i}{4}(H_{+0} - H_{0+} - H_{-0} + H_{0-})$	$\frac{-i}{2\sqrt{2}}(H_{31} - H_{13})$	$\frac{3}{\sqrt{2}}\sin\theta\sin\chi$
H_F	$H_{++} - H_{--}$	$-i(H_{12} - H_{21})$	$\frac{3}{4}\cos\theta$
H_A	$\frac{1}{4}(H_{+0} + H_{0+} + H_{-0} + H_{0-})$	$\frac{-i}{2\sqrt{2}}(H_{23} - H_{32})$	$\frac{-3}{\sqrt{2}}\sin\theta\cos\chi$
H_4	$-\frac{i}{2}(H_{+-} - H_{-+})$	$-\frac{1}{2}(H_{12} + H_{21})$	$-\frac{3}{4}\sin^2\theta\sin 2\chi$
H_5	$-\frac{i}{4}(H_{+0} - H_{0+} + H_{-0} - H_{0-})$	$\frac{-1}{2\sqrt{2}}(H_{23} + H_{32})$	$\frac{3}{2\sqrt{2}}\sin 2\theta\sin\chi$

Table 1

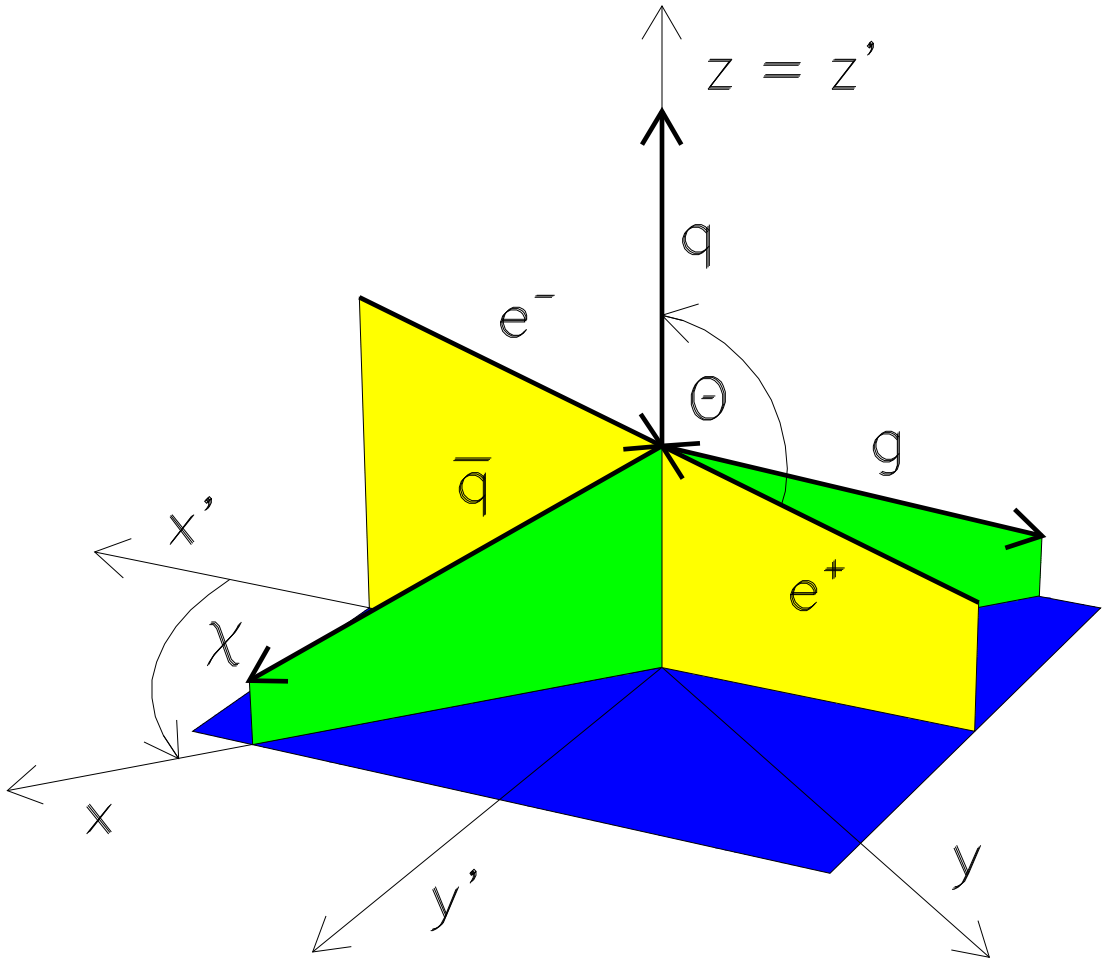

Figure 1

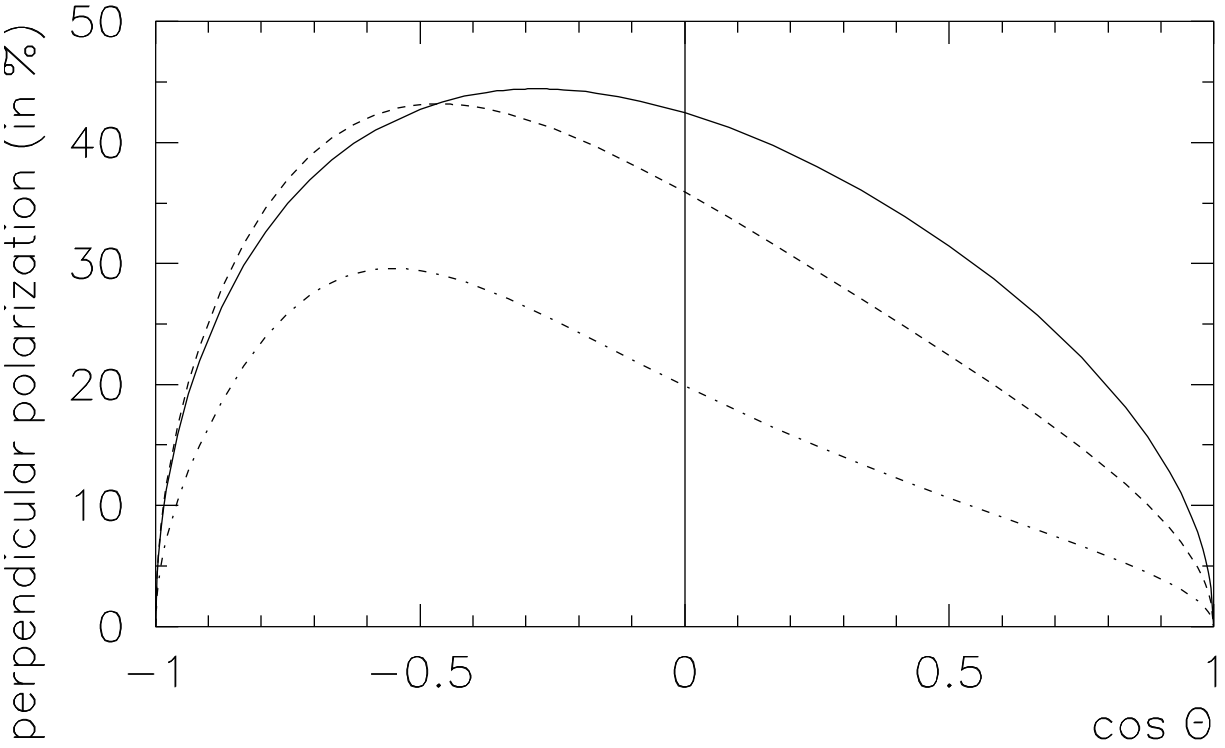

Figure 2(a)

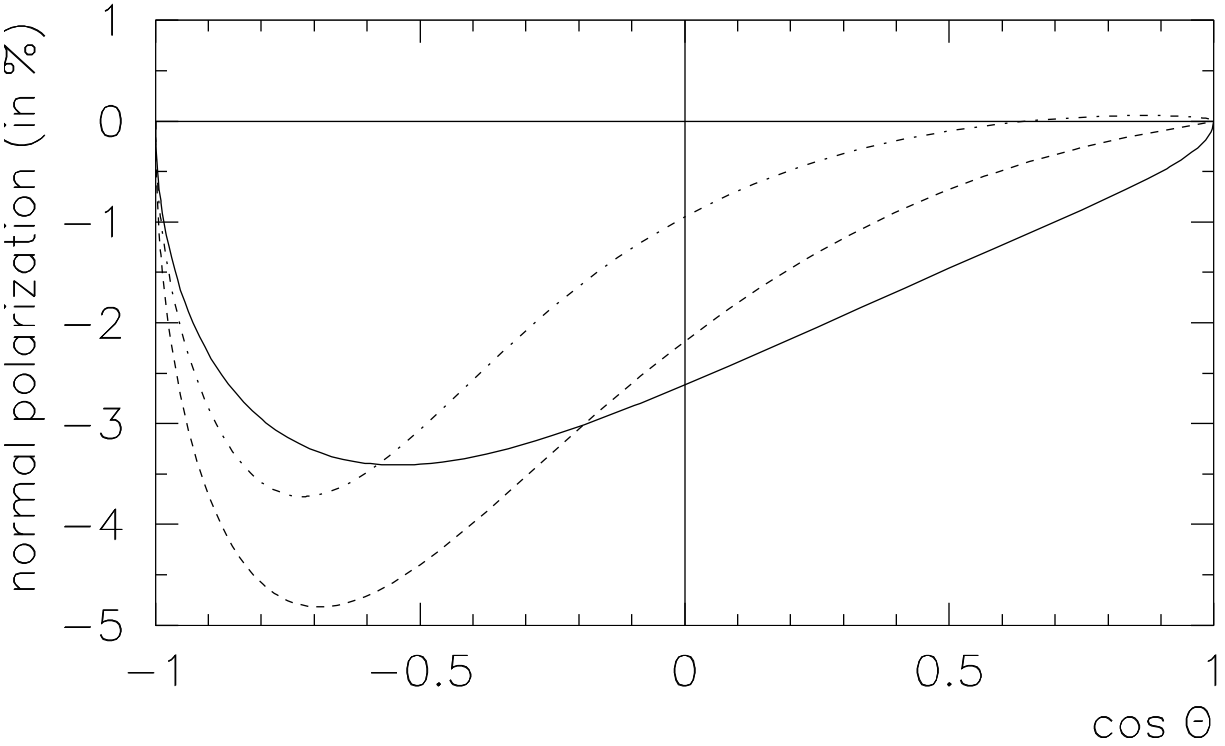

Figure 2(b)

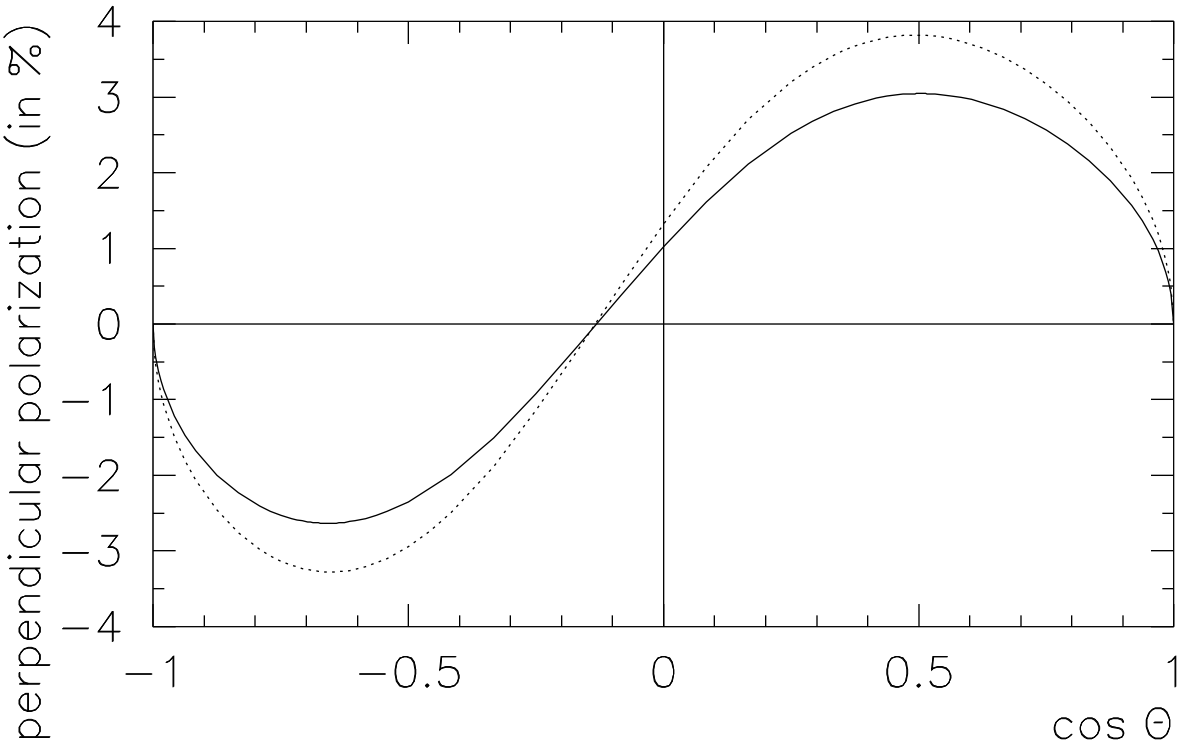

Figure 3(a)

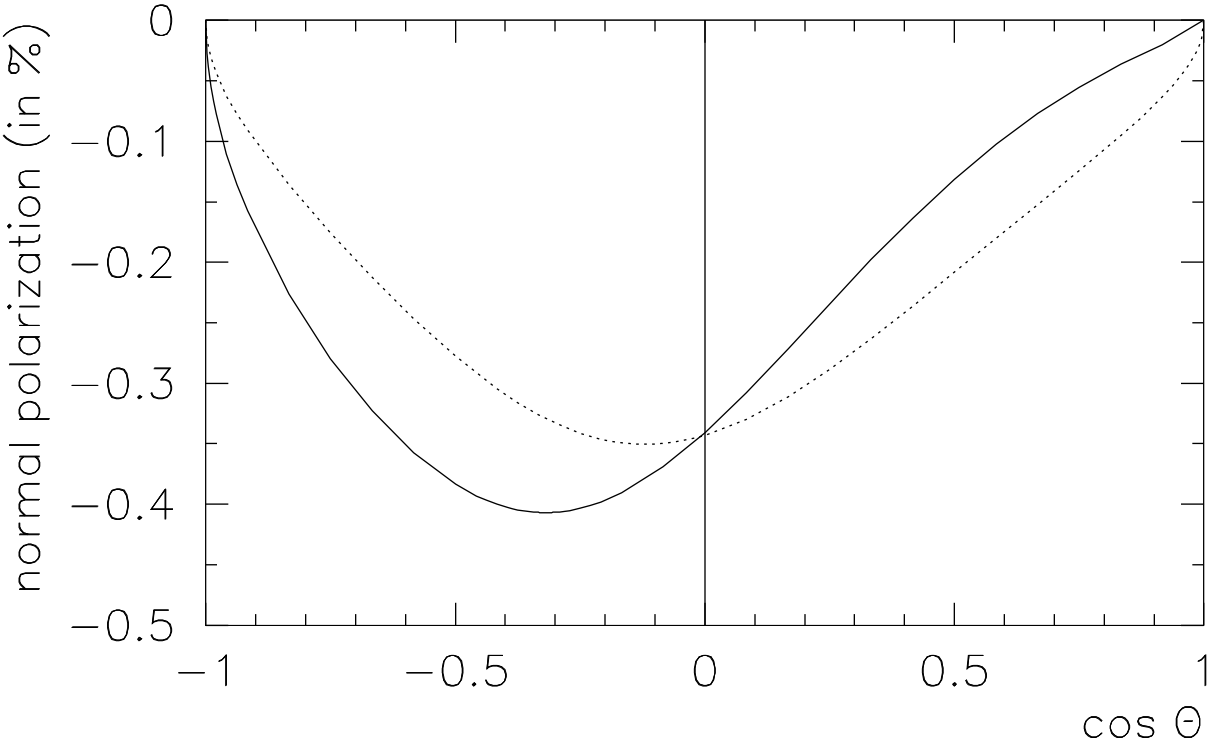

Figure 3(b)